Thermal analysis of asynchronous machines under intermittent loading

Z. Vondrášek, V. Ryženko[*], M. Linda

Czech University of Life Sciences Prague, Faculty of Engineering, Kamýcká 129, CZ165 21 Prague, Czech Republic
[*]Correspondence: ryzhenko@tf.czu.cz

Abstract. The operation of electric machines is accompanied by losses which are mostly converted to heat. The heat needs to be dissipated from the machine. With a properly dimensioned motor, the arising heat is balanced with dissipated one. After the motor is started at ambient temperature, all functional parts of the machine are gradually warmed until stabilized. Any overloading of the machine leads to stabilization at temperatures higher than expected by the designers. High temperatures in the machine could cause a crash by damaging an insulation. In case of machines with permanent magnets, the temperature affects their magnetic properties and can leads to demagnetization at the Curie temperature. Therefore, the measuring of temperature is so important for verifying the allowed warming of the motor. Contact and noncontact methods could be used for temperature measuring. Thermal warming and temperature distribution in an electric machine can be also determined by theoretical calculations based, for example, on the finite element method. This method is used by a number of computer software such as Ansys. The article deals with generation and propagation of heat in electric motors and with measuring of warming characteristics with a variable value of a load factor for intermittent periodic loading of asynchronous machine. The loading is carried out by the dynamometer. The temperature measurement is implemented by temperature sensors which are located on the stator winding of the asynchronous motor and are in operation for the whole time the motor is loaded.

Key words: electric machine, loading, losses, load factor, warming.

INTRODUCTION

Asynchronous motors are among the most common nowadays, due to fact that they are the simplest, and at the same time the most reliable motors without the need for frequent maintenance. During operation, heat caused by friction or electricity conduction is generated throughout various parts of the asynchronous motor. This heat then gradually expands (from its place of origin) towards the surface of the motor, where it is being leaked into ambient (Staton & Šušnjić, 2009). Not all the heat however is dispersed and part of it remains inside of the motor.

Material out of which the motor is constructed plays a major role. Just like any other object, asynchronous motors have their own exponential curve of heating and cooling. Slow application of load to the motor gradually increases its temperature to the point of reaching the maximal steady warm-up value. As the motor speeds up during start-up sequence from zero to nominal values, it consumes a notably greater amount of

electricity than during normal operation. In a matter of seconds, the temperature of rotor and stator winding increases considerably. This is caused by the fact that during this short amount of time the surrounding iron did not manage to increase its temperature high enough to be able to conduct and radiate the heat. Therefore it is imperative to take into consideration the amount of time the motor needs to start up, during which the thermal protection should not be triggered. The heat transfer in the asynchronous motor under no-load and different cooling conditions is discussed by Gedzurs (2014).

Higher operating temperatures shorten lifespan of individual parts as well as the entire motor. Reasons of exceeding motor's operating temperatures could be high frequency of power-ups, locked rotor or failure of power supply phase etc. This is why the thermal protection of motors should be constructed in a way to protect all of its sensible components from high temperatures for which the machine and its components are not dimensioned (Pawlus et al., 2017). The different modes of motor operation (overload, locked rotor, too frequent or prolonged acceleration etc.) are discussed for example in Venkataraman et al. (2005).

At the same time, the motor must not be disconnected during spool-up or spool-down sequence. Cooling system that removes generated heat, which consequently lowers the stress caused by high temperatures is therefore one of the most important parts of the motor, directly prolonging its overall lifespan (Staton et al., 2005). Cooling systems can be divided into three types: natural cooling, self-cooling and artificial cooling. Natural cooling is characterized by the motor conducting thermal energy to space (convection) without the use of a ventilator or coolant. Self-cooling motors have a ventilator unit placed on their operating shaft which brings cool air from the surrounding area to the motor. Artificial cooling consist of a ventilator that is completely independent of the motor's operating shaft and, as a result, the motor is still being cooled even if in idle state.

In diagnostics, temperature is one of the most important values, and has to be taken into consideration during revisions and inspections of electrical motors. With the help of temperature it is possible to determine whether the motor works according to its requirements and parameters, or if there has been a malfunction. High temperature can cause damage to the motor's isolation, which may result in its failure (Kosmodamianskii et al., 2011). Magnetic properties of motors with permanent magnets can be affected by high temperatures. Reaching Curie's temperature may cause their demagnetization. Taking measurements of electric motors under applied load plays an important role in their electromagnetic dimensioning. This is to check the correctness of previous design and the motor's properties under special conditions.

MATERIALS AND METHODS

The load factor z is defined as a ratio of the loading duration t_z to the period $T = t_z + t_0$ (see Fig. 1). As a loading device was used the 1DS541N dynamometer manufactured by MEZ Vsetin. Its schedule power is 18 kW for generator mode and 14.7 kW for motor mode. It allows measurement at a maximum rotational speed of 8,000 rpm and a torque peak of 80 Nm. It is a DC machine with a swinging stator. The forces applied on the swinging stator during the machine's operation are transmitted to a force meter with scale. The force meter is calibrated in torque units. The power

supply of the DC machine is realized by a Ward-Leonard rotary converter, type 1DP642-4. The converter consists of asynchronous and DC machines. It is designed as a mono-block.
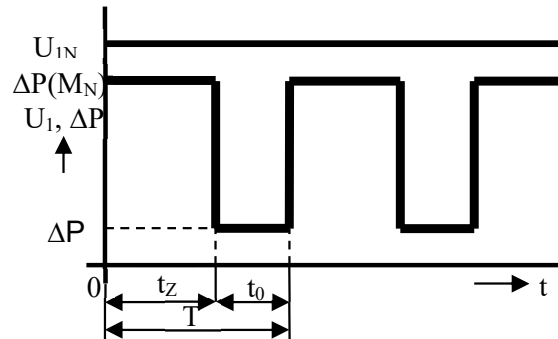
The asynchronous motor has a power of 22 kW, 1455 rpm and is connected to a three-phase distribution network 3x380 V, 50 Hz. It starts as a motor using the Y / Δ switch. It can work both as a motor and as a generator. The DC machine has a power output of 16.5 kW, 1500 rpm. Its rotor circuit parameters are 230 V, 71.7 A, the excitation circuit voltage is up to 220 V.

After starting the dynamometer and the asynchronous motor the nominal values of the motor voltage were set. The asynchronous motor was connected via a clutch to a dynamometer. For temperature measurements we used 4 K type thermocouples with low time constant in order to capture the rapid temperature change with sufficient accuracy.
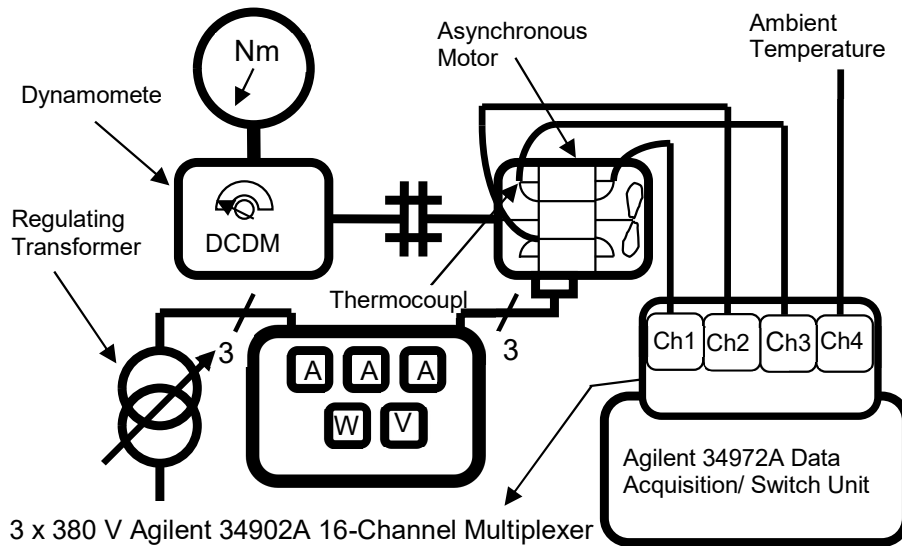

Figure 1. Time diagram of intermittent load of asynchronous motor at constant terminal voltage $U_1 = U_{1N}$. T [min] – motor load cycle time; t_z [min] – motor running time with defined loading; t_0 [min] – motor idle running time; $\Delta P(M)$ [W] – total losses of asynchronous motor at defined load; ΔP_0 [W] – overall losses of asynchronous motor during idle operation; M_N – motor load under nominal current I_{1N}.

In the motor stator winding, three thermocouples have been attached to points 1−3, which are located at different places in order to display temperature differences of the motor components. Thermocouple number 4 was used to measure an ambient air temperature. These thermocouples are composed of NiCr (+) and NiAl (-). The thermocouple outputs were connected via the connectors to the Agilent 34972A Data Acquisition / Switch Unit via the Agilent 34902A 16-Channel Multiplexer.

The circuit was connected according to the wiring diagram, see Fig. 2. Temperature recording was done automatically in 2s − intervals and measured data was automatically saved on the Flash storage device. The resulting temperature values were graphically plotted as temperature characteristics $\theta = f(t)$.

For measuring of heating of the asynchronous motor during its operation, it is necessary to know its main operation modes. Standard ČSN EN 60034-1 distinguishes between 10 modes of operation according to international classification. With respect to the given limitations of carrying out the test, two representative loading modes were selected. The first one is continuous operation of the motor at its nominal load, marked as S1.

Figure 2. Measuring scheme.

The tested device is 4AP100L-2 induction motor with performance 3 kW. The load was applied using the 1DS541N dynamometer. The motor was started and the voltage set to the nominal value of 380 V (line-to-line). Subsequently, the dynamometer was activated and the load torque set to 8 Nm; during such a load the motor consumes the current around the nominal value of 6.2 A. The asynchronous motor is designed to run with such continuous load value. The test was run for 50 minutes in order to determine the limit operating temperature of selected winding parts – namely at the front end winding, near the front shield at the fan (sensor 1), at the rear shield at the outlet of the winding from groove (near the shaft; sensor 2) and at the rear end winding (sensor 3). During the measurement however, the normalized ambient temperature of 40 °C was not maintained. To simplify the theory, the motor is replaced by a homogeneous body with the same temperature in all parts. In our case, this assumption does not apply on the whole motor, but to the parts of the winding whose heating is monitored. For the physical description of the thermal processes of the motor, it is necessary to define the following quantities according to Petrbok et al. (1985):

m [kg] - weight of a monitored part;

c [J K^{-1} kg^{-1}] – the specific heat capacity of the material of the parts;

α [W m^{-2} K^{-1}] – heat transfer coefficient;

S [m^2] – surface of the monitored part;

ϑ [°C] – temperature of the monitored part;

ϑ_0 [°C] – ambient temperature;

ΔP [W] – power dissipation in the defined part.

From these quantities the thermal time constant τ_{th} is derived as:

$$\tau_{th} = \frac{m \cdot c}{\alpha \cdot S} \tag{1}$$

Warming:

$$\Delta\vartheta = \vartheta - \vartheta_o \tag{2}$$

1249

In each monitored part of the motor the power dissipation is converted to the heat according to the equation:

$$dQ_\Delta = \Delta P \cdot dt \quad\quad (3)$$

This heat is partually move through the surface of the monitored part into the environment:

$$dQ_{konv} = \alpha \cdot S \cdot (\vartheta - \vartheta_o) \cdot dt, \quad\quad (4)$$

and partially increase the temperature of the mentioned above part according to:

$$dQ_{th} = m \cdot c \cdot d\vartheta \qu\quad (5)$$

The energy balance of the monitored part is described by the differential equation:

$$dQ_\Delta = dQ_{konv} + dQ_{th} \qu\quad (6)$$

$$\Delta P \cdot dt = \alpha \cdot S \cdot (\vartheta - \vartheta_o) \cdot dt + m \cdot c \cdot d\vartheta \qu\quad (7)$$

This differential equation is solved by separating of variables:

$$\Delta P \cdot dt - \alpha \cdot S \cdot (\vartheta - \vartheta_o) \cdot dt = m \cdot c \cdot d\vartheta \qu\quad (8)$$

The warming is given by the equation:

$$\{\Delta P - \alpha \cdot S \cdot (\vartheta - \vartheta_o)\} \cdot dt = m \cdot c \cdot d\vartheta \qu\quad (9)$$

At steady state ($t \to \infty$), the warming is

$$\Delta\vartheta = \Delta\vartheta_\infty = \frac{\Delta P}{\alpha \cdot S} \qu\quad (10)$$

The temperature of the monitored part varies continuously according to the next equation:

$$\Delta\vartheta = \frac{\Delta P}{\alpha \cdot S} - K \cdot e^{-\frac{t}{\tau_{th}}} \qu\quad (11)$$

The integrating constant K can be determined from the boundary conditions for t = 0, where the warming is $\Delta\vartheta = 0$.

Similar behavior of the monitored part can be expected during the cooling process. Differences occur in two cases. If the motor is disconnected during cooling from the source, there is no heat loss. In this case the motor stops and the cooling occurs only by natural convection and radiation. It is easier to determine the steady state as the motor temperature returns to the same level as its surroundings. A different situation applies for instances of intermittent load. During cooling, the motor is not disconnected from the power supply and it is running idle. This way the losses are reduced by the square of the consumed current. This is the second measured case of intermittent load motor load with different load factors according to ČSN EN 60034-1, marked as S6. The described operating mode is similar to the operation of machine tools. During the load, the generated losses cause the motor to heat up gradually, as with a constant load.

RESULTS AND DISCUSSION

The main aim of this research was to find the highest rate of motor heating during operation. Asynchronous motor has exponential dependence of the heating with time. The motor was loaded with torque of 8 Nm; hereby the motor consumed nominal current of 6.18 A. During the idle run, the average current was 2.77 A, i.e. 44.6% of the nominal

current. The losses in the winding decrease with the square of the current, here to about 20% of the original value. The motor was loaded in 10-minute cycles with different load factors from the initial state (disconnected from the power supply) when the motor temperature was the same as in its surroundings. The selected load factor levels were 20%, 40%, 60% and 80%. As was mentioned above, the normalized ambient temperature of 40 °C was not applied, but fluctuated, specifically between 24 and 27 °C.

In total, 7 cycles for each load factor value were performed. During the cyclic loading, saw-toothed course of the temperature was observed, as can be seen in the graphs in Figs. 3–6.
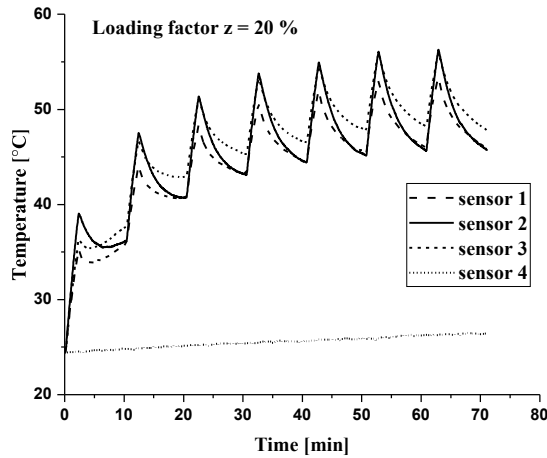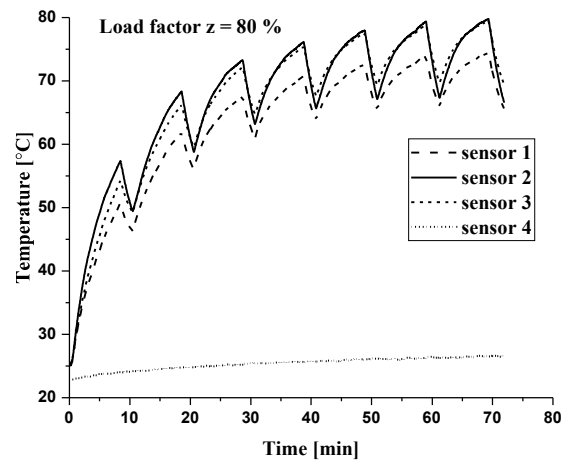
Figure 3. Time course of temperature of the observed asynchronous motor stator winding parts, and of the nearby air under 20% motor load factor.
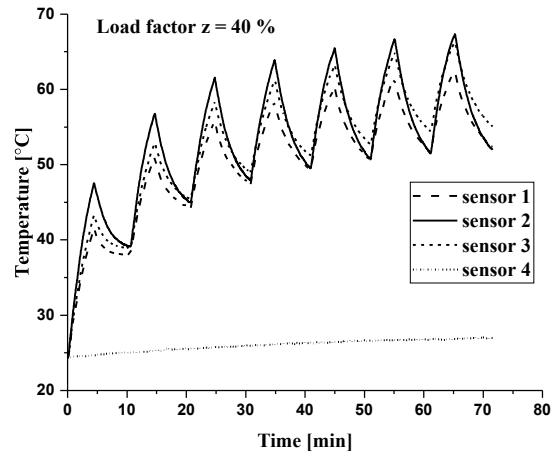
Figure 4. Time course of temperature of the observed asynchronous motor stator winding parts, and of the nearby air under 40% motor load factor.
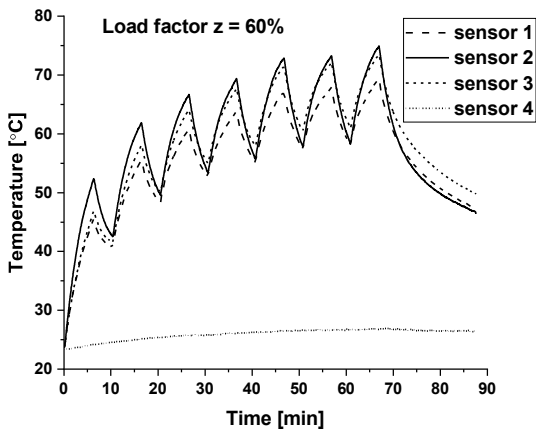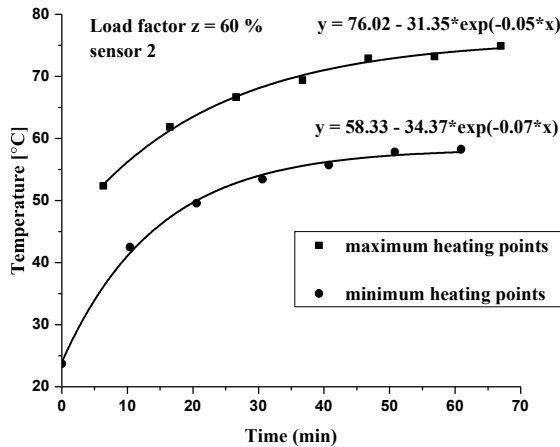
Figure 5. Time course of temperature of the observed asynchronous motor stator winding parts, and of the nearby air under 60% motor load factor and its cool-down during the motor idle running (after 66 min.).
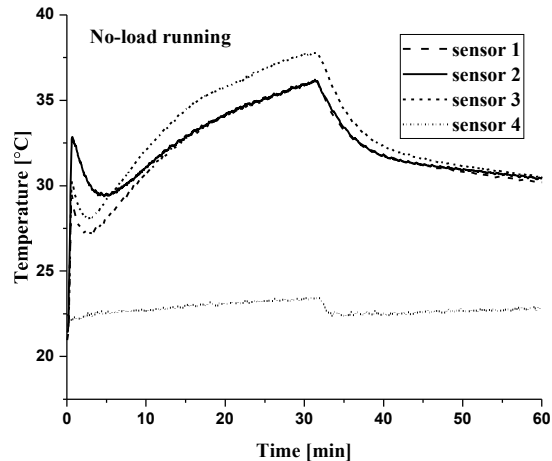
Figure 6. Time course of temperature of the observed asynchronous motor stator winding parts, and of the nearby air under 80% motor load factor.

Basing on the temperature course, for each load factor value and for each temperature sensor, respective regression curves can be determined; the boundary points of the warming and cooling characteristics lie on this regression curve (see Fig. 7).

One of the objectives of the research was an idle running asynchronous motor heating test. The time course of temperature of the observed asynchronous motor stator winding parts, and of the nearby air during the motor's idle state after direct nominal voltage start-up (during 30 minutes) and its cool-down after power supply disconnection (during 30 minutes) can be seen in the graph in Fig. 8.


Figure 7. Envelope of individual maximal and minimal heating points (with approximate functions) of the asynchronous motor winding, measured by sensor 2 under 60% motor load factor.

Figure 8. Time course of temperature during the motor's idle state after direct nominal voltage start-up and its cool-down after power supply disconnection (rotor stationary).

The start of the asynchronous motor was implemented by its direct connection to the power supply. It was also the current impulse in the stator winding that was transferred to the rotor winding. In spite of a short-term duration of the above-mentioned impulse, the rotor cage winding is likely to be heavily heated. The heat radiation from the cage winding affected the temperature of sensor 2 as did the motor running under load. The impact of the heat emission was greater than the heat dissipation from the stator winding to the cold ferromagnetic circuit. After the effect of the current impulse during the motor start finished, the originally hot parts cooled down as a result of the heat transfer to the cold ferromagnetic circuit. Subsequently, it was sensor 3 that recorded the highest temperatures on the rear winding face. The rear face of the winding can be cooled down only by air. As there was no air exchange with the environment, the heating of the rear winding face was faster than in the ferromagnetic circuit.

Fig. 9. shows the time course of temperature of the observed asynchronous motor stator winding parts, and of the nearby air under constant nominal motor load. The resulting maximal temperature at the end of the monitored running time was approximately 81 °C.
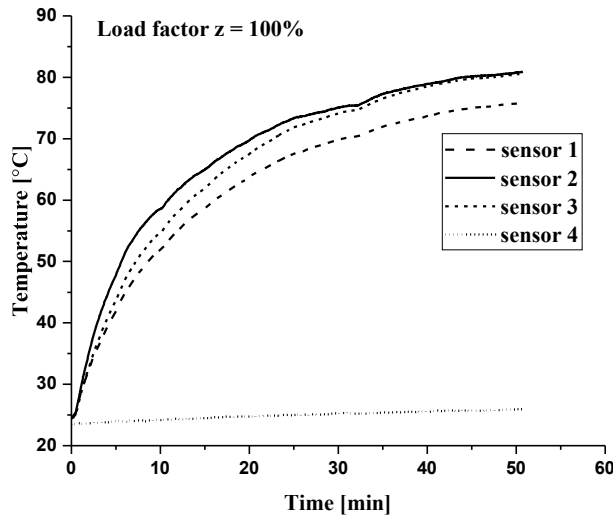
Figure 9. Time course of temperature of the observed asynchronous motor stator winding parts, and of the nearby air under constant nominal motor load.

CONCLUSIONS

As is apparent from the measurements, applying intermittent load on the asynchronous motor leads to lower heat stress of its electrical circuits. An important finding is the possibility of the use of insulation materials for achieving lower operating temperatures. When using more thermally resilient insulants of motor windings, and applying intermittent load, it is possible to securely overload the motor. It is important to take into consideration the increasing power losses with the second power of motor's current drawn. By comparing the changes in temperature of the individual motor winding segment, it was found that at the place of winding groove output located at the opposite side from the ventilator experiences the highest fluctuations in temperature. This is most apparent during motor load up to 60%.

Detected deviation from the expected high temperature fluctuations, at the front of the winding that faces away from the ventilator, is most likely caused by the fact that the winding conductors are not placed as close to each other. The thermal sensor therefore is not heated as intensively as it is in the place of winding output. Mentioned sensor is located at the side of the winding's air gap. It can be partially affected by heat radiating from the ring of the rotor's cage winding.

The rings and the outer parts of the rotor winding rods are according to O.Badran et al. (2012) the most heated components of the motor during its operation. In the case of the front part of the motor winding, at the side of the ventilator was temperature the lowest. This is caused by the presence of the ventilator, which intensively cools down the motor's surface, and therefore easily removes generated heat from this part of the motor.

Another finding indicates that in the case of 80% motor load, the maximal observed temperature of motor winding parts reach similar values as of motors running on maximal load. Possible structural savings are in this case negligible.

REFERENCES

Badran, O., Sarhan, H. & Alomour, B. 2012. Thermal performance analysis of induction motor. *International Journal of Heat and Technology* **30**(1), 75–88.

ČSN EN 60034-1 ed.2 Rotating electrical machines - Part 1: Rating and performance. 2011.

Gedzurs, A. 2014. Heating of low-power induction motor under no-load mode and different cooling conditions. In: *Research for rural development 2014: annual 20th international scientific conference proceedings* **1**, Latvia University of Agriculture. Jelgava: LLU, pp. 219.-224.

Kosmodamianskii, A. S., Vorobiev, V. I. & Pugachev, A. A. 2011. The Temperature Effect on the Performance of a Traction Asynchronous Motor. *Elektrotekhnika* **8**, 50–54.

Pawlus, W., Khang, H.V. & Hansen, M.R. 2017. Temperature Rise Estimation of Induction Motor Drives Based on Loadability Curves to Facilitate Design of Electric Powertrains. *IEEE Transactions on Industrial Informatics* **13**(3), pp. 985–994.

Petrbok, K., Pokorný, K. & Klíma, J. 1985. Electrical Engineering and Electrification II. Czech University of Life Sciences, Prague, 108 pp (in Czech).

Staton, D., Boglietti, A. & Cavagnino, A. 2005. Solving the More Difficult Aspects of Electric Motor Thermal Analysis in Small and Medium Size Industrial Induction Motors. *IEEE Transactions on Energy Conversion* **20**(3), 620–628.

Staton, D. & Šušnjić, L. 2009. Induction Motors Thermal Analysis. *Strojarstvo* **51**(6), 623-631.

Venkataraman, B., Godsey, B., Premerlani, W., Shulman, E., Thakur, M. & Midence, R. 2005. Fundamentals of a Motor Thermal Model and its Applications in Motor Protection. In: *Proceeding of the 58th Annual Conference for Protective Relay Engineers*. College Station, TX, pp. 127–144.